Field measurements of gasoline direct injection emission factors: spatial and seasonal variability

Naomi Zimmerman, Jonathan M. Wang, Cheol-Heon Jeong, Manuel Ramos, Nathan Hilker, Robert M. Healy, Kelly Sabaliauskas, James S. Wallace, and Greg J. Evans

Field measurements of gasoline direct injection emission factors: spatial and seasonal variability

Naomi Zimmerman,[†] Jonathan M. Wang, [†] Cheol-Heon Jeong, [†] Manuel Ramos, [‡]

Nathan Hilker, [†] Robert M. Healy, [†] Kelly Sabaliauskas, [†] James S. Wallace, [‡] Greg J. Evans[†,]*

[†]Department of Chemical Engineering and Applied Chemistry, University of Toronto, Toronto, Ontario M5S3E5 Canada

[‡] Department of Mechanical and Industrial Engineering, University of Toronto, Toronto, Ontario M5S3G8 Canada

Corresponding author:
Dr. Greg J. Evans
Dept. of Chemical Engineering and Applied Chemistry
University of Toronto
200 College Street, Room 127, Toronto, Canada, M5S 3E5
Tel. 416-978-1821
Fax. 416-978-8605

Email: greg.evans@utoronto.ca

KEYWORDS

Gasoline direct injection, real-world, fuel-based, vehicle, emission factors, ultrafine particles, black carbon, volatility, size distribution

TOC/Abstract Art:

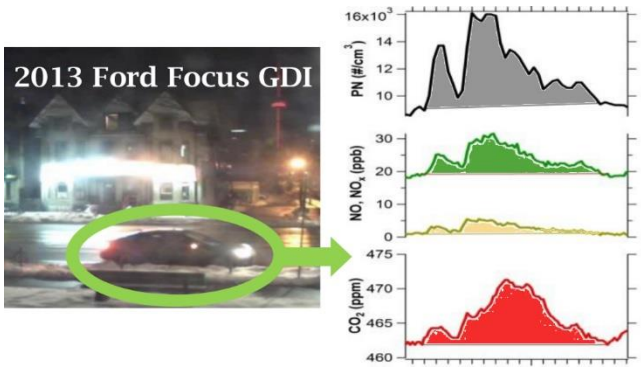

ABSTRACT

Four field campaigns were conducted between February 2014 and January 2015 to measure emissions from light-duty gasoline direct injection (GDI) vehicles (2013 Ford Focus) in an urban near-road environment in Toronto, Canada. Measurements of CO_2, CO, NO_x, black carbon (BC), benzene, toluene, ethylbenzene-xylenes (BTEX), and size-resolved particle number (PN) were recorded 15 m from the roadway and converted to fuel-based emission factors (EFs). Other than for NO_x and CO, the GDI engine had elevated emissions compared to the Toronto fleet, with BC and BTEX EFs in the 80-90th percentile, and PN EFs in the 75th percentile during wintertime measurements. Additionally, for three campaigns, a second platform for measuring PN and CO_2 was placed 1.5-3 m from the roadway to quantify changes in PN with distance from point of emission. GDI vehicle PN EFs were found to increase by up to 240% with increasing distance from the roadway, predominantly due to an increasing fraction of sub-40 nm particles. PN and BC EFs from the same engine technology were also measured in the laboratory. BC EFs agreed within 20% between the laboratory and real-world measurements; however, laboratory PN EFs were an order of magnitude lower due to exhaust conditioning.

1. INTRODUCTION

In the United States, the Corporate Average Fuel Economy (CAFE) standards have specified a minimum fuel economy of 37.8 mpg by 2016[1,2], with similar fuel economy regulations set in Canada and Europe. The CAFE standard will continue to increase by 5% per year until 2025, when minimum fuel economy must exceed 55 mpg. In response to these stringent regulatory requirements on passenger vehicle fuel economy, automobile manufacturers have been increasingly turning to gasoline direct injection (GDI) engines, which offer up to a 25% improvement in fuel economy compared to port fuel injection (PFI) engines[3]. Market share of GDI vehicles is increasing rapidly; between model years 2009 and 2014 there was a ten-fold increase in GDI engine sales[4], and it is projected that in 2016 the market share of new light-duty vehicles with this technology will exceed 50%[5].

Compared to PFI-equipped vehicles, GDI-equipped vehicles emit substantially more particulate matter (PM)[6–9] due to incomplete fuel volatilization causing fuel impingement on cylinder and piston surfaces and incomplete fuel mixing with air resulting in pockets of fuel rich combustion. Particle size distributions from GDI engine exhaust have generally been observed to be either bimodal[10–13], unimodal[9,14–16], or vary[7,17] depending on factors such as engine operation, ethanol fuel content, and fuel injection system. Of the observed bimodal size distributions, the smaller mode is typically <25 nm and has been proposed to be dominated by soot cores[11,18] or semi-volatile nucleation particles[13,19]; however, their composition remains highly uncertain. There is stronger consensus that the larger mode, typically 40-100 nm, is composed of agglomerated soot particles with adsorbed semi-volatile material that has condensed.

Accurately characterizing GDI PM also presents a measurement challenge; compared to diesel, the large aromatic fraction in gasoline is expected to produce PM with a larger organic mass fraction and with higher volatility[20–22]. As such, GDI PM mass loadings and chemical composition may vary depending on the measurement environment or exhaust conditioning. For example, two laboratory measurements of GDI organic carbon (OC) using the same measurement technique but different dilution systems resulted in measured organic carbon mass fractions (OC:PM ratios) ranging from <0.25 to 0.57[9,23].

Recent computational fluid dynamic models of diesel exhaust behaviour in exhaust plumes have suggested that as the plume dilutes in the "tailpipe-to-road" region, the combination of sulfuric acid, water vapor, condensable organics and soot particles results in rapidly growing particles within the exhaust plume.[24–26] This growth may also occur in GDI exhaust plumes, since particle number (PN) emissions have been shown to be influenced by sulfur content in lubricating oil[27], but the time scales for these growth processes are unknown and this effect has not yet been directly measured. Given the projected increase in GDI vehicle market share in the coming years, an improved understanding of the characteristics and variability of GDI emissions in both laboratory and real-world near-road environments is needed to guide legislation and support emissions models and inventories. Additionally, gas phase organic emissions from gasoline vehicles are known precursors to secondary organic aerosol (SOA) in urban areas[28–30], thus measuring GDI emissions in near-road environments may contribute to our understanding of how GDI vehicles impact PM in urban environments.

In this study, GDI emissions, expressed as fuel-based emission factors (EFs), were evaluated in an urban near-road environment during four campaigns conducted between February 2014 and January 2015 spanning a broad range of meteorological conditions. PN EFs were also measured at distances ranging from 1.5-15 m from the roadway to quantify spatial variability. Additionally, particle number (PN) and black carbon (BC) EFs were compared to laboratory measurements performed in a manner similar to the European Union Particle Measurement Program (PMP)[31] (i.e., removal of volatile fraction through heated dilution) to quantify the differences between the two measurement environments.

2. METHODS

2.1 Measurement Site

Emission factor measurements were made during four campaigns carried out between February 2014 and January 2015 at the Southern Ontario Centre for Atmospheric Aerosol Research (SOCAAR) Field Measurement Facility in downtown Toronto, Canada. The sampling site is located north of a four-lane roadway that experiences relatively high traffic volumes ranging from 16,000 – 25,000 cars per day[32]. Due to the high traffic volumes, all measurements were taken from 3:00AM – 6:00AM when traffic volume was at a minimum to isolate the signal from the GDI vehicle and eliminate the effects of photochemistry. Measurements were taken across a total of 11 days and grouped by season: winter 2014, spring 2014, summer 2014, and winter 2015. During each set of measurements, wind speed, wind direction, temperature, and relative humidity were also recorded concurrently with a Vaisala WXT520 Weather Transmitter located 3 m above ground. The measurement campaigns captured a broad range of meteorological conditions, with

106 temperatures and relative humidity ranging from -7.5°C to +17.5°C and 53.2 to 93.7%,
107 respectively. Specific details of measurement dates, times, and meteorological conditions are
108 provided in the Supporting Information.

109

110 **2.2 Field research vehicles and operation**

111 Field measurements were taken from 2013 Ford Focus light-duty SE sedans equipped with
112 gasoline direct injection (GDI) engines fuelled with commercially-available gasoline. A single
113 vehicle model was used as a control to explore the impacts of season, meteorology, vehicle
114 operation, and distance from roadway on emissions. While measurements from additional GDI-
115 equipped vehicles would be beneficial, this was outside the scope of this specific study and will
116 be explored in future work. The vehicles were rented from a local car sharing service. To ensure
117 emissions from the vehicle were not affected by poor engine tuning or the need for vehicle
118 maintenance, a total of seven unique 2013 Ford Focus vehicles were used across the 11
119 measurement days. For the winter 2014 and spring 2014 campaigns a 2000 Honda CR-V equipped
120 with a PFI engine was also deployed to compare GDI and PFI PN emissions. The vehicles were
121 operated under three conditions: 1) engine idle, 2) cruising at 40 km/h, and 3) acceleration from
122 20 km/h to 50 km/h. Emissions from braking were not considered due to the possibility of PN
123 emissions occurring independent of CO_2 emissions.[33] Vehicle speed and location were recorded
124 with an on-board diagnostics (OBD2) data logger (Mini ELM327 V1.5) and driveway reflector
125 rods were installed at the roadside to ensure the vehicle was stopping, starting, and idling at a
126 consistent location across all measurement days. Prior to recording any emissions from the test
127 vehicles, the vehicles were warmed up for a minimum of 20 minutes. During the measurement

periods, the vehicles remained on at all times to ensure the engine remained at its set operating temperature. Emissions measured from City of Toronto garbage trucks (predominantly diesel fleet) passing the measurement site during the campaigns were also recorded. A graphical representation of the measurement site is provided in the Supporting Information (Figure S1).

2.3 Measurement Techniques

A detailed description of the instrumentation at the SOCAAR field measurement facility has been reported previously[32], but is summarized briefly here. At the SOCAAR measurement site ("near-road site"), inlets sampling ambient air were located 15 m from the roadway and 3 m above ground to measure NO, NO_x, CO, CO_2 (Thermo Scientific 42i, 48C, and 410i), benzene, toluene, and ethylbenzene-xylenes (BTEX, IONICON Analytik PTR-TOF-MS), particle number (PN) concentration (TSI CPC 3788) and size distribution (TSI FMPS 3090), and black carbon (BC, Droplet Measurement Technologies PASS-3). For the spring 2014, summer 2014, and winter 2015 measurement campaigns, a second measurement station to measure CO_2 and PN concentration and size distribution was constructed 3 m from the roadway and 1 m above ground ("roadside site") to measure any spatial variability in particle phase emissions during plume dilution. During the winter 2015 campaign, a 1.5 m inlet line was added to the secondary measurement station and extended forwards enabling an additional measurement 1.5 m from the roadway. A summary of the instrumentation and deployment is provided in the Supporting Information.

2.4 Data Analysis

The algorithm and validation protocols developed in Wang et al.[32] were applied in IGOR Pro v6.34 to automatically identify vehicle exhaust plumes based on inflection points in the CO_2 time series

and to calculate vehicle EFs. As part of this protocol, pollutant signals were time synchronized, and we considered only plumes with a minimum time-integrated peak area of 20 mg C-s m-3. Plumes shorter than 10 s or with an average carbon content less than 2 mg C m^{-3} were rejected. Instrument sensitivities were calculated from the measured signal during vehicle-free periods. Measured plumes with pollutant signals below this sensitivity (i.e., CO_2 signal but no significant pollutant signal) were classified as "below threshold" (BT) and were calculated using the effective sensitivity in the numerator of Equation (1). A detailed discussion of calculating instrument sensitivity and applying instrument sensitivity to EF calculations is provided in Wang et al.[32] For above threshold (AT) pollutant signals, fuel-based EFs were calculated according to Equation (1).

$$\mathrm{EF_P} = \left(\frac{\Delta[\mathrm{P}]}{\Delta[\mathrm{CO_2}]+\Delta[\mathrm{CO}]}\right) w_{\mathrm{C}} \qquad (1)$$

Where EF_P is the fuel-based emission factor of pollutant P (in g, mg, or particle number) per kg of fuel burned assuming ambient conditions (25°C, 101.325 kPa). In equation (1), ΔP, ΔCO_2, and ΔCO are the background subtracted concentrations integrated across the plume duration, and w_c is the weight fraction of carbon in gasoline fuel (assumed $w_c = 0.86$).[34] For the "roadside site" no CO measurement was available, and as such the CO term was removed from equation (1); however, the bulk of the fuel carbon is assumed to be converted to CO_2 and the calculated CO_2:CO ratio at the near-road site exceeded 1000. Additionally, the GDI vehicles were recent models all with very low mileage (<50,000 km) expected to produce a very low CO signal because of the young catalyst. While the Honda CR-V was not a recent model, near-road (15 m) CO emissions were detected from less than 30% of the plumes at levels at or below the fleet average calculated in Wang et al.[32]

Prior to calculating emission factors, some post-processing of the particle number and size distribution measurements was performed. As measurements of vehicle exhaust with an FMPS or

174 EEPS instrument have been shown to result in over counting of PN and misclassification of particle
175 size[35], the correction protocol described in Zimmerman et al.[36] was applied here. Additionally,
176 the data were corrected for line losses, thermodenuder transmission efficiency (where applicable),
177 and differences in CPC cut-off diameters. Further information on the instrument time resolution,
178 detection limits, and data correction are included in the Supporting Information.
179

180 **2.5 Laboratory Measurement of Particle Phase Emissions**

181 Elemental carbon (EC) and PN EFs were also calculated from laboratory measurements taken
182 using a 2012 Ford Focus 2.0L displacement wall-guided naturally aspirated GDI engine coupled
183 to an engine dynamometer. While the laboratory engine was one model year older than the vehicles
184 used for the real-world testing, they are nominally the same engine. The laboratory engine was
185 operated at a steady-state highway cruise condition (2600 rpm, 41 ft-lb) representative of highway
186 driving at approximately 100 km/h in top gear. The engine was fuelled with commercially-
187 available premium gasoline (91 anti-knock index / 95 research octane number) containing no
188 ethanol, denoted E0, and commercially-available premium gasoline splash blended with
189 anhydrous ethanol to make a 10% (v/v) ethanol blend, denoted E10. An E10 fuel was tested
190 because in Ontario, regular gasoline (87 anti-knock index) must contain at least 5% (v/v) ethanol[37],
191 with many suppliers selling fuel containing up to 10% (v/v) ethanol.

192 Details of engine operation, tests fuels, a schematic of the engine laboratory sampling
193 configuration, details of the thermal-optical transmittance protocol and calculation of EC
194 concentration, and details of EF calculations with the laboratory data set is provided in the
195 Supporting Information.

3. RESULTS AND DISCUSSION

3.1 Emission Factor Detection and Classification

Plume capture was defined based on total CO_2 within the plume. If a pollutant concentration in a captured plume was below the effective instrument thresholds (see Table S3, Supporting Information) then the pollutant EF was designated "below threshold" (BT). Across the measurement campaigns, a plume was captured (i.e., CO_2 signal detected) at the near-road (15 m) and roadside (3 m) sites 46% and 71% of the time the GDI vehicle passed the site, respectively. This amounted to a total of 93 plumes detected at the near-road site and 61 plumes at the roadside site. The absolute number of captured roadside plumes was less than near-road plumes as the roadside site was not deployed during the winter 2014 campaign. The percentage of plumes below threshold varied by pollutant, but in general ranged from 20-40% for NO_x, PN, BC, and VOCs and ranged from 65-90% for CO. From the meteorological data, EFs were only detected when ground level winds were blowing towards the inlet, which was located north of the roadway. A summary of capture rate by pollutant and by driving condition, and the wind rose of detected plumes is provided in the Supporting Information.

Seasonal differences in EFs were found to be of greater significance than differences in vehicle operation and vehicle ID, thus EFs were averaged across all driving conditions. A Welch's two-sided t-test for differences between driving conditions (see Supporting Information, Table S7) indicated that differences in emission factors by driving condition were largely statistically insignificant. While there is consensus that driving condition should impact vehicle emission factors, the small sample size for each driving condition and high degree of variability from the single vehicle real-world measurement method did not allow for a meaningful assessment of the

218 impact of vehicle operation. Additionally, there was little difference in the shape of the plume-
219 averaged particle size distributions for each of the vehicle operating conditions (provided in the
220 Supporting Information).

221 **3.2 Emission Factors at the Near-Road (15 m) Site**

222 The above threshold and combined (above threshold and below threshold) EFs from the near-road
223 (15 m) site were averaged seasonally. Pollutants which varied seasonally included PN and BTEX,
224 whereas NO_x, CO, and BC showed no distinct seasonality (Welch's t-test $p > 0.1$, all p-values
225 reported in Supporting Information). Furthermore, CO was not detected in significant quantities
226 in the GDI exhaust, as expected for a relatively new vehicle with a young catalyst.

227

228 The combined PN EFs ranged from 4.13 – 11.3 $x10^{14}$ particles kg-$fuel^{-1}$ and were inversely
229 correlated with outdoor air temperature; average near-road (15 m) PN EFs in winter 2015 were 2.7
230 and 1.8 times larger than the EFs measured in spring and summer 2014, respectively. Average
231 temperature vs. average PN EF is provided in the Supporting Information. Cooler outdoor
232 temperature may impact PN emissions in two ways: increased gas-to-particle partitioning of low
233 volatility gases[38–40] and a prolonged cold start condition increasing PN emissions[7,41,10]. An
234 exception to this trend was observed during the summer 2014 campaign. While temperatures
235 during the summer 2014 campaign exceeded those during the spring 2014 campaign, the detected
236 PN EFs were 48% higher in summer 2014. This is potentially due to the seasonal changes in fuel
237 formulation (i.e., summer grade vs winter grade) to achieve a target Reid vapor pressure. In
238 summer grade fuel, the volatility is reduced by replacing n-butane with heavier alkanes and
239 aromatic hydrocarbons including toluene.[42,43] Increasing gasoline fuel aromatic content has been

shown to increase soot formation in engine laboratory studies. For example, doping commercially-available fuel with 10% toluene resulted in a 112% increase in BC concentration [44] and increasing fuel aromatic content from 15% to 25% resulted in a 78% and 169% increase in BC and PN emissions, respectively.[45] In this study, BTEX emissions, especially ethylbenzene-xylenes, were elevated in the exhaust in summer 2014 relative to spring 2014 and above detection threshold levels of toluene were detected in the plumes 20% more often relative to other seasons (see Supporting Information).The broad range of BTEX emissions likely reflects variability in the aromatics found in commercial gasoline blends, which vary by supplier and season. The test vehicles came pre-fuelled, thus variability is expected to be maximized.

Figure 1 shows the GDI vehicle EFs overlaid on a cumulative probability distribution of the Toronto fleet EFs from the same measurement site originally reported in Wang et al.[32] from four month-long continuous campaigns performed between November 2013 and September 2014. For NO_x, the campaign-averaged EFs from the GDI were in line with the Toronto fleet average (NOx: 52nd percentile of the fleet). Compared to the Toronto fleet, on average the GDI vehicle produced PN emission factors in the 52nd percentile of the fleet; however, this varied by season (range: 45th percentile in spring 2014 to 75th percentile in winter 2015). For BC, compared to the Toronto fleet the campaign-averaged GDI vehicle EFs were in the 85th percentile, suggesting that as GDI vehicles penetrate the market, ambient BC levels may rise substantially. As of late 2014, only 17% of the Toronto fleet had detectable BC emissions[32], and these emissions have been largely attributed to heavy-duty diesel vehicles. Within the above detection threshold fleet emissions, the GDI vehicle BC EFs were in the 18th percentile, suggesting that the GDI vehicle has BC emissions slightly lower than the on-road diesel fleet. This is in agreement with laboratory studies, which

have measured BC EFs from diesel vehicles as 3-7 times higher than GDI vehicles[46–51]. However, as the share of on-road diesel vehicles with diesel particulate filters increases, it is expected that GDI vehicles may become the dominant source of ambient BC and PN. The BTEX EFs from the GDI vehicle were also substantially higher compared to the Toronto fleet (range: 58th to 98th percentile) suggesting that GDI vehicles may also increase ambient BTEX levels; these species are soot precursors and may be incomplete combustion products from the vehicle. Furthermore, fuel-rich operation during vehicle transients or fuel-rich pockets within the cylinder, noted issues with GDI vehicles[10,52,53], have been shown to increase BTEX emissions[54], potentially explaining the elevated emissions relative to the Toronto fleet. An important caveat to this analysis is that both Toronto fleet and GDI vehicle EFs were calculated on a fuel burned basis. On a distance travelled basis, the relative impact of GDI emissions would be reduced due to the improvement in fuel economy. For example, by comparing the reported city driving fuel economies of first generation (2004, PFI), second generation (2008, PFI) and third generation (2013, GDI) Ford Focus vehicles, it can be estimated that replacing a first generation and second generation Ford Focus with a third generation GDI vehicle would result in a 23% and 13% improvement in city driving fuel economy, respectively[55–57]. However, the observed increases in BC, BTEX, and in some seasons PN with the GDI vehicle used in this study relative to the current Toronto fleet is expected to outweigh the benefits from improved fuel economy.

3.3 Near-road vs. Roadside Particle Number Emission Factors

For the GDI vehicle, PN emission factors were found to exhibit a strong degree of spatial variability. Mean PN EFs at 15 m from the roadway were up to 300% higher than EFs at 1.5 m from the roadway (Figure 2). This micro-scale spatial variability was highest in the winter and

smallest in the summer, indicating that the relative increase in particle emissions is influenced by ambient temperature. In comparison, based on the spring 2014 campaign measurements of the port fuel injected CRV, the average PN EFs exhibited less spatial variability, with mean PN EFs 15 m from the roadway 17% lower than those measured 3 m from the roadway (all PN EFs are available in the Supporting Information).

The EFs in Figure 2 are average values across all driving and meteorological conditions, and thus the confidence intervals are large due to the range of PN EFs measured. To further explore the micro-scale spatial variability, the ratio of the PN EFs at 15 m and 3 m was calculated on a plume-by-plume basis for the spring 2014, summer 2014, and winter 2015 measurement campaigns (Figure 3). Only plumes where PN emissions were above the detection threshold at both the roadside site and then subsequently the near-road site were considered. To determine if spatial variability in PN emissions in the near-road environment was unique to GDI PM, plume-by-plume ratios were also calculated for the PFI vehicle in spring 2014 and for detected garbage truck plumes across all the measurement campaigns; garbage trucks are predominantly diesel vehicles which typically emit a strong PN signal.

On a plume-by-plume basis, GDI PN EFs were 130 – 240% higher 15 m than 3 m from the roadside, depending on season. Differences were at a minimum during the summer campaign (warmest campaign) and at a maximum during the winter 2015 campaign (coldest campaign) indicating that condensation may play an important role in GDI exhaust PM dynamics. In the near-road (15 m) region, nucleation, condensation/evaporation, coagulation, and pollutant dilution may all affect the measured PN EF at different distances from the roadway. As CO_2 and particles have different diffusion coefficients, assuming PN EFs are constant in the near-road environment

309 requires advection to be the dominant mass transport process. This was verified by calculating
310 Peclet numbers for wind speeds ranging from 0.25 – 10 m/s and for 1.5 – 15 m from the roadway
311 (details in Supporting Information). In all cases, Peclet numbers were several orders of magnitude
312 above unity, indicating that advection is indeed dominant and spatial/temporal changes in PN EFs
313 are likely due to chemical or physical processing of the exhaust aerosol in the atmosphere.
314 Additionally, for the garbage trucks and the PFI vehicle, no spatial variability was observed, i.e.,
315 differences in PN emission factors at 3 and 15 m were statistically insignificant using a Welch's t-
316 test (garbage trucks: $p = 0.64$, PFI: p-value = 0.65). Size resolved PFI PN EFs, as well as a complete
317 discussion of the garbage truck plumes used as a control in this study, are provided in the
318 Supporting Information.
319

320 Size-resolved GDI PN EFs for each of the campaigns are shown in Figure 4. These size
321 distributions were bimodal, consistent with several previous studies[10–13], and the distributions from
322 the 2014 and 2015 winter campaigns were broader than those measured in the spring and summer
323 2014 campaigns. Further, the upper mode was larger in the winter; 100 nm in winter vs 40-55 nm
324 in spring and summer campaigns, likely due to increased condensation in the colder outdoor
325 temperatures and limited nighttime mixing conditions. Comparing the PN EF size distributions
326 from the near-road (15 m) and the roadside (1.5 – 3 m) measurement sites, it was observed that
327 across all measurement campaigns there was a net increase in PN EF and growth in the mode
328 diameter in the lower sub-40 nm mode region. Additionally, the increase in sub-40 nm particles
329 15 m from the roadway was less pronounced during the summer 2014 campaign, possibly due to
330 the competing effects of evaporation in the warmer weather. This is in contrast to the upper mode
331 region (40-100 nm), where the near-road PN EFs were higher between 3 and 15 m from the

roadway for the spring and summer campaigns but with no net change in the shape of the distribution. This could be affected by seasonal differences in background semi-volatile compound concentrations; however, these were not measured and thus this finding remains unclear. Thermodenuded particle size distributions (Supporting Information Figure S7) were generally bimodal with modes at 10 and 25 nm, suggesting the semi-volatile components within the exhaust or in the background air may strongly influence the final measured size distribution.

Considering the sub-40 region separately there may be two possible effects on PN EFs: (1) rapid growth of small particles below instrument detection limits (<5 nm) via condensation of low volatility gases to form new sub-40 nm particles and (2) coagulation of particles resulting in particle growth and a less distinct bimodality. The latter mechanism is unlikely due to the small coagulation coefficient between two sub-6 nm particles; while these very small particles have high velocities, the probability of collision is low due to their limited cross-sectional area.[58] In order for the former effect to be true, a substantial concentration of exhaust particles below the instrument cut off (6 nm) are required as a core for condensational growth. A recent study demonstrated that 2 nm amorphous carbon particles are readily formed at flame temperatures in the GDI combustion chamber[59], potentially acting as condensation nuclei and influencing gas-particle partitioning.

Increasing PN EFs in the 15 m near-road region were not observed for the PFI vehicle, which is also expected to produce low volatility organic vapours capable of condensing onto existing soot cores. Here, we suggest two reasons for this observation: a lower concentration of soot cores from the tailpipe of PFI vehicles and a volatility distribution of PFI vehicles shifted towards higher vapour pressure compounds (i.e., more volatile). In GDI vehicles, there is less time for fuel

vaporization and air-fuel mixing, resulting in a less homogeneous fuel charge (i.e., fuel rich pockets in the combustion chamber) and greater liquid fuel impingement on cylinder surfaces compared to PFI vehicles.[60,61] These areas of rich combustion are expected to result in the formation of incomplete combustion products including soot and SVOCs[62]. While May et al.[63] conclude that all gasoline vehicles emit primary organic aerosol with a similar volatility distribution, the GDI vehicle included in their study was excluded from the reported volatility distribution due to contamination of the dynamic blanks, thus the differences in volatility distribution between PFI and GDI vehicles remains unclear. In this study, comparing winter 2014 and spring 2014 near-road PN EFs, there was a statistically significant increase from spring to winter of 125% for the GDI vehicle ($p=0.022$), while the observed increase in PN EF from the PFI vehicle was not statistically significant ($p=0.18$). Assuming this increase is primarily due to condensation, the larger relative increase with the GDI vehicle suggests a greater degree of gas-particle partitioning for the GDI vehicle in the near-road region compared to PFI. In the Supporting Information, the concentration of organic vapor needed to achieve the observed GDI PM growth rates is explored; however, the mechanism for the observed near-road dynamics remains unclear. As such, future studies of GDI PM particle formation and growth mechanisms are recommended to better understand our findings.

3.4 Laboratory and Real-World Comparison

PN EFs measured in the real-world were observed to exceed those measured in the laboratory by approximately an order of magnitude (Figure 2 vs. Figure 5). Measurements in real-world environments are diluted naturally in the atmosphere, where the volatile fraction can contribute significantly to the PN concentration. The large discrepancy between the real-world and laboratory

particle number emissions has important regulatory implications, since the sub-23 nm fraction of the PM is not considered in European regulations, but may have significant air quality implications or contribute to the formation of secondary organic aerosol.

Removing the volatile fraction of the real-world exhaust PM with a thermodenuder (T=250°C) should result in PN EFs that can be directly compared to the laboratory, as the exhaust will have undergone similar pretreatment. Comparing thermodenuded real-world PN EFs to the laboratory PN EFs resulted in particle number emission factors that agreed with laboratory measurements within approximately 30% (Figure 5). As the engine was operated at a simulated highway cruise condition in the laboratory, PN EFs in the laboratory may be slightly higher due to the higher engine load and speed as compared to driving in an urban environment.

Laboratory and real-world BC emission factors were also compared as an internal control for the real-world-based method. Exhaust conditioning and meteorology are expected to have minimal impacts on black carbon, which is atmospherically stable, and as such, laboratory and real-world measurements should be in agreement. Black carbon (real-world) and elemental carbon (laboratory) emission factors were also comparable (Figure 5); compared to the summer 2014 campaign, real-world BC EF agreed with the E10 laboratory elemental carbon emission factors within 10%. This is consistent with the requirement in Ontario that regular gasoline (87 anti-knock index) contain at least 5% (v/v) ethanol and with many suppliers providing fuel with up to 10% (v/v) ethanol. While differences between laboratory elemental carbon and real-world BC can be affected by the thermal-optical and photoacoustic methods[64,65], we used site-specific mass absorption cross-section (MAC) values to ensure close agreement between the two methods.

401

402 **3.5 Implications**

403 From this study, it can be concluded that particles in GDI vehicles have PN, BC, and BTEX EFs
404 in the upper end of the fleet distribution and the exhaust plumes exhibit dynamic behaviour in the
405 near-road (15 m) region, with increasing PN EFs at increasing distance from the roadway. This
406 suggests that as GDI vehicle market penetration increases, there may be negative impacts on local
407 air quality, especially in urban environments near roadways. The observed near-road PN dynamics
408 were unique to GDI vehicles, as the same effects were not observed for heavy-duty diesel garbage
409 trucks or a PFI-equipped vehicle. From comparing GDI vehicle size distributions at different
410 distances from the roadway, rapid particle growth of sub-5 nmcores due to condensation of low
411 volatility organic gasses is proposed to be the dominant growth mechanism in GDI vehicle exhaust.
412 Given the rapid integration of GDI-equipped vehicles, understanding the impacts of GDI vehicles
413 on local and regional air quality presents a significant measurement challenge, because exhaust
414 PN and BTEX concentrations were found to be strongly influenced by meteorological conditions.
415 Additionally, the current European regulatory practice for quantifying exhaust PN, which only
416 considers non-volatile PN larger than 23 nm, appears to be ill-suited to this exhaust type; PN EFs
417 with no thermal pretreatment were approximately an order of magnitude larger than non-volatile
418 PN laboratory measurements. Furthermore, the dynamics investigated in this study were limited
419 to 15 m from the roadway. Understanding the fate of GDI vehicle exhaust beyond 15 m remains
420 an important research question, and the potential for GDI vehicle exhaust to form secondary
421 organic aerosol relative to PFI vehicle exhaust is currently unknown. Going forward, there is a
422 need to explore GDI emissions from more vehicles to better quantify the effect on vehicle fleet
423 emissions, and to understand the longer term behaviour of GDI vehicle exhaust in real-world
424 settings through more detailed experiments, aerosol aging studies, and micro-scale modelling.

ACKNOWLEDGEMENTS

Funding for this study was provided by the Canadian Foundation for Innovation (CFI 19606) and the Natural Sciences and Engineering Research Council (NSERC) Strategic Project Grant program (STPGP 396488-10). N. Zimmerman's funding was provided by the NSERC Postgraduate Scholarship. M. Ramos's funding was provided by the AUTO21 Network of Centres of Excellence (Project D506-DMP). The authors thank C. Maikawa and A. Rodrigues for their assistance monitoring the roadside instruments.

SUPPORTING INFORMATION

Further details on the study methodology, instrumentation and method validation, statistical testing, tabulated emission factors, size distributions and an analyses of emissions growth dynamics are provided.

References

(1) United States Department of Transportation. *Final regulatory impact analysis, corporate average fuel economy for MY 2012-MY 2016 passenger cars and light trucks*; Washington, D.C., 2010.

(2) United States Environmental Protection Agency. 2017 and later model year light-duty vehicle greenhouse gas emissions and corporate average fuel economy standards; final rule. *Fed. Regist.* **2012**, *77* (199), 62624–63200.

(3) Zhao, F.; Lai, M. C.; Harrington, D. L. Automotive spark-ignited direct-injection gasoline engines. *Prog. Energy Combust. Sci.* **1999**, *25* (5), 437–562.

(4) United States Environmental Protection Agency. *Light-duty automotive technology , carbon dioxide emissions , and fuel economy trends : 1975 through 2014*; 2014.

(5) United States Environmental Protection Agency. *Final rulemaking to establish light-duty vehicle greenhouse gas emission standards and corporate average fuel economy*

standards; 2010.

(6) Graham, L. Chemical characterization of emissions from advanced technology light-duty vehicles. *Atmos. Environ.* **2005**, *39* (13), 2385–2398.

(7) Khalek, I. A.; Bougher, T.; Jetter, J. J. Particle emissions from a 2009 gasoline direct injection engine using different commercially available fuels. *SAE Int. J. Fuels Lubr.* **2010**, *3* (2), 623–637.

(8) Liang, B.; Ge, Y.; Tan, J.; Han, X.; Gao, L.; Hao, L.; Ye, W.; Dai, P. Comparison of PM emissions from a gasoline direct injected (GDI) vehicle and a port fuel injected (PFI) vehicle measured by electrical low pressure impactor (ELPI) with two fuels: Gasoline and M15 methanol gasoline. *J. Aerosol Sci.* **2013**, *57*, 22–31.

(9) Maricq, M. M.; Szente, J. J.; Jahr, K. The impact of ethanol fuel blends on PM emissions from a light-duty GDI vehicle. *Aerosol Sci. Technol.* **2012**, *46* (5), 576–583.

(10) Peckham, M. S.; Finch, A.; Campbell, B.; Price, P.; Davies, M. T. Study of particle number emissions from a turbocharged gasoline direct injection (GDI) engine including data from a fast-response particle size spectrometer. In *SAE 2011 World Congress and Exhibition*; 2011.

(11) Barone, T. L.; Storey, J. M. E.; Youngquist, A. D.; Szybist, J. P. An analysis of direct-injection spark-ignition (DISI) soot morphology. *Atmos. Environ.* **2012**, *49*, 268–274.

(12) Sementa, P.; Maria Vaglieco, B.; Catapano, F. Thermodynamic and optical characterizations of a high performance GDI engine operating in homogeneous and stratified charge mixture conditions fueled with gasoline and bio-ethanol. *Fuel* **2012**, *96*, 204–219.

(13) Karjalainen, P.; Pirjola, L.; Heikkilä, J.; Lähde, T.; Tzamkiozis, T.; Ntziachristos, L.; Keskinen, J.; Rönkkö, T. Exhaust particles of modern gasoline vehicles: A laboratory and an on-road study. *Atmos. Environ.* **2014**, *97*, 262–270.

(14) Storey, J. M.; Barone, T.; Norman, K.; Lewis, S. Ethanol Blend Effects On Direct Injection Spark-Ignition Gasoline Vehicle Particulate Matter Emissions. *SAE Int. J. Fuels Lubr.* **2010**, *3* (2), 650–659.

(15) Chan, T. W.; Meloche, E.; Kubsh, J.; Rosenblatt, D.; Brezny, R.; Rideout, G. Evaluation

of a Gasoline Particulate Filter to Reduce Particle Emissions from a Gasoline Direct Injection Vehicle. *SAE Int. J. Fuels Lubr.* **2012**, *5* (3), 1277–1290.

(16) Chen, L.; Stone, R.; Richardson, D. Effect of the valve timing and the coolant temperature on particulate emissions from a gasoline direct-injection engine fuelled with gasoline and with a gasoline-ethanol blend. *Proc. Inst. Mech. Eng. Part D J. Automob. Eng.* **2012**, *226* (10), 1419–1430.

(17) Zhang, S.; McMahon, W. Particulate Emissions for LEV II Light-Duty Gasoline Direct Injection Vehicles. *SAE Int. J. Fuels Lubr.* **2012**, *5* (2), 637–646.

(18) Sgro, L. A.; Sementa, P.; Vaglieco, B. M.; Rusciano, G.; D'Anna, A.; Minutolo, P.; D'Anna, A.; Minutolo, P. Investigating the origin of nuclei particles in GDI engine exhausts. *Combust. Flame* **2012**, *159* (4), 1687–1692.

(19) Mathis, U.; Mohr, M.; Forss, A.-M. Comprehensive particle characterization of modern gasoline and diesel passenger cars at low ambient temperatures. *Atmos. Environ.* **2005**, *39* (1), 107–117.

(20) United States Environmental Protection Agency. *Analysis of particulate matter emissions from light-duty gasoline vehicles in Kansas City*; 2008.

(21) Cadle, S. H.; Mulawa, P. A.; Hunsanger, E. C.; Nelson, K.; Ragazzi, R. A.; Barrett, R.; Gallagher, G. L.; Lawson, D. R.; Knapp, K. T.; Snow, R. Composition of light-duty motor vehicle exhaust particulate matter in the Denver, Colorado area. *Environ. Sci. Technol.* **1999**, *33* (14), 2328–2339.

(22) Robinson, A. L.; Grieshop, A. P.; Donahue, N. M.; Hunt, S. W. Updating the conceptual model for fine particle mass emissions from combustion systems. *J. Air Waste Manage. Assoc.* **2010**, *60* (10), 1204–1222.

(23) Storey, J. M. E.; Lewis, S.; Szybist, J. P.; Thomas, J.; Barone, T. L.; Eibl, M.; Nafziger, E.; Kaul, B. Novel characterization of GDI engine exhaust for gasoline and mid-level gasoline-alcohol blends. *SAE Int. J. Fuels Lubr.* **2014**, *7* (2), 571–579.

(24) Uhrner, U.; Zallinger, M.; von Löwis, S.; Vehkamäki, H.; Wehner, B.; Stratmann, F.; Wiedensohler, A. Volatile nanoparticle formation and growth within a diluting diesel car exhaust. *J. Air Waste Manage. Assoc.* **2011**, *61* (4), 399–408.

(25) Olin, M.; Rönkkö, T.; Dal Maso, M. CFD modeling of a vehicle exhaust laboratory sampling system: sulfur-driven nucleation and growth in diluting diesel exhaust. *Atmos. Chem. Phys.* **2015**, *15* (9), 5305–5323.

(26) Wang, Y. J.; Zhang, K. M. Coupled turbulence and aerosol dynamics modeling of vehicle exhaust plumes using the CTAG model. *Atmos. Environ.* **2012**, *59*, 284–293.

(27) Pirjola, L.; Karjalainen, P.; Heikkilä, J.; Saari, S.; Tzamkiozis, T.; Ntziachristos, L.; Kulmala, K.; Keskinen, J.; Rönkkö, T. Effects of fresh lubricant oils on particle emissions emitted by a modern gasoline direct injection passenger car. *Environ. Sci. Technol.* **2015**, *49* (6), 3644–3652.

(28) Gentner, D.; Isaacman, G.; Worton, D. R.; Chan, A. W. H.; Dallmann, T. R.; Davis, L.; Liu, S.; Day, D. A.; Russell, L. M.; Wilson, K. R.; et al. Elucidating secondary organic aerosol from diesel and gasoline vehicles through detailed characterization of organic carbon emissions. *Proc. Natl. Acad. Sci.* **2012**, *109* (45), 18318–18323.

(29) Goldstein, A. H.; Galbally, I. E. Known and unknown organic constituents in the Earth's atmosphere. *Environ. Sci. Technol.* **2007**, *41* (5), 1514–1521.

(30) Nordin, E. Z.; Eriksson, a. C.; Roldin, P.; Nilsson, P. T.; Carlsson, J. E.; Kajos, M. K.; Hellén, H.; Wittbom, C.; Rissler, J.; Löndahl, J.; et al. Secondary organic aerosol formation from idling gasoline passenger vehicle emissions investigated in a smog chamber. *Atmos. Chem. Phys.* **2013**, *13* (12), 6101–6116.

(31) Giechaskiel, B.; Chirico, R.; Decarlo, P. F.; Clairotte, M.; Adam, T.; Martini, G.; Heringa, M. F.; Richter, R.; Prevot, A. S. H.; Baltensperger, U.; et al. Evaluation of the particle measurement programme (PMP) protocol to remove the vehicles' exhaust aerosol volatile phase. *Sci. Total Environ.* **2010**, *408* (21), 5106–5116.

(32) Wang, J. M.; Jeong, C.-H.; Zimmerman, N.; Healy, R. M.; Wang, D. K.; Ke, F.; Evans, G. J. Plume-based analysis of vehicle fleet air pollutant emissions and the contribution from high emitters. *Atmos. Meas. Tech.* **2015**, *8* (8), 3263–3275.

(33) Rönkkö, T.; Pirjola, L.; Ntziachristos, L.; Heikkilä, J.; Karjalainen, P.; Hillamo, R.; Keskinen, J. Vehicle engines produce exhaust nanoparticles even when not fueled. *Environ. Sci. Technol.* **2014**, *48* (3), 2043–2050.

(34) Ban-Weiss, G. A.; Lunden, M. M.; Kirchstetter, T. W.; Harley, R. A. Size-resolved particle number and volume emission factors for on-road gasoline and diesel motor

vehicles. *J. Aerosol Sci.* **2010**, *41* (1), 5–12.

(35) Zimmerman, N.; Godri Pollitt, K. J.; Jeong, C.-H.; Wang, J. M.; Jung, T.; Cooper, J. M.; Wallace, J. S.; Evans, G. J. Comparison of three nanoparticle sizing instruments: The influence of particle morphology. *Atmos. Environ.* **2014**, *86*, 140–147.

(36) Zimmerman, N.; Jeong, C.-H.; Wang, J. M.; Ramos, M.; Wallace, J. S.; Evans, G. J. A source-independent empirical correction procedure for the Fast Mobility and Engine Exhaust Particle Sizers. *Atmos. Environ.* **2015**, *100*, 178–184.

(37) Ontario Environmental Protection Act. O. Reg. 535/05: Ethanol in Gasoline. 2007.

(38) Ranjan, M.; Presto, A. A.; May, A. A.; Robinson, A. L. Temperature dependence of gas–particle partitioning of primary organic aerosol emissions from a small diesel engine. *Aerosol Sci. Technol.* **2012**, *46* (1), 13–21.

(39) Charron, A.; Harrison, R. M. Primary particle formation from vehicle emissions during exhaust dilution in the roadside atmosphere. *Atmos. Environ.* **2003**, *37* (29), 4109–4119.

(40) Janhäll, S.; Molnar, P.; Hallquist, M. Traffic emission factors of ultrafine particles: effects from ambient air. *J. Environ. Monit.* **2012**, *14* (9), 2488–2496.

(41) He, X.; Ratcliff, M. A.; Zigler, B. T. Effects of gasoline direct injection engine operating parameters on particle number emissions. *Energy & Fuels* **2012**, *26* (4), 2014–2027.

(42) Lough, G. C.; Schauer, J. J.; Lonneman, W. A.; Allen, M. K. Summer and Winter Nonmethane hydrocarbon emissions from on-road motor vehicles in the midwestern United States. *J. Air Waste Manage. Assoc.* **2005**, *55* (5), 629–646.

(43) White, M. L.; Russo, R. S.; Zhou, Y.; Ambrose, J. L.; Haase, K.; Frinak, E. K.; Varner, R. K.; Wingenter, O. W.; Mao, H.; Talbot, R.; et al. Are biogenic emissions a significant source of summertime atmospheric toluene in rural Northeastern United States? *Atmos. Chem. Phys. Discuss.* **2008**, *8* (3), 12283–12311.

(44) Ramos, M. Sources of Particulate Matter Emissions Variability from a Gasoline Direct Injection Engine, MASc. Thesis, University of Toronto, Toronto, Canada, 2014.

(45) Karavalakis, G.; Short, D. Z.; Vu, D.; Russell, R. L.; Hajbabaei, M.; Asa-Awuku, A.; Durbin, T. D. Evaluating the effects of aromatics content in gasoline on gaseous and

particulate matter emissions from SI-PFI and SI-DI vehicles. *Environ. Sci. Technol.* **2015**, *49*, 7021–7031.

(46) Forestieri, S. D.; Collier, S.; Kuwayama, T.; Zhang, Q.; Kleeman, M. J.; Cappa, C. D. Real-time black carbon emission factor measurements from light duty vehicles. *Environ. Sci. Technol.* **2013**, *47* (22), 13104–13112.

(47) Park, S. S.; Kozawa, K.; Fruin, S.; Mara, S.; Hsu, Y. K.; Jakober, C.; Winer, A.; Herner, J. Emission factors for high-emitting vehicles based on on-road measurements of individual vehicle exhaust with a mobile measurement platform. *J. Air Waste Manag. Assoc.* **2011**, *61* (10), 1046–1056.

(48) Hudda, N.; Fruin, S.; Delfino, R. J.; Sioutas, C. Efficient determination of vehicle emission factors by fuel use category using on-road measurements: downward trends on Los Angeles freight corridor I-710. *Atmos. Chem. Phys.* **2013**, *13* (1), 347–357.

(49) Gëller, M. D.; Sardar, S. B.; Phuleria, H.; Fine, P. M.; Sioutas, C. Measurements of particle number and mass concentrations and size distributions in a tunnel environment. *Environ. Sci. Technol.* **2005**, *39* (22), 8653–8663.

(50) Westerdahl, D.; Wang, X.; Pan, X.; Zhang, K. M. Characterization of on-road vehicle emission factors and microenvironmental air quality in Beijing, China. *Atmos. Environ.* **2009**, *43* (3), 697–705.

(51) Liggio, J.; Gordon, M.; Smallwood, G.; Li, S.-M.; Stroud, C.; Staebler, R.; Lu, G.; Lee, P.; Taylor, B.; Brook, J. R. Are emissions of black carbon from gasoline vehicles underestimated? Insights from near and on-road measurements. *Environ. Sci. Technol.* **2012**, *46* (9), 4819–4828.

(52) Storey, J. M. E.; Barone, T. L.; Thomas, J. F.; Huff, S. P. Exhaust particle characterization for lean and stoichiometric DI vehicles operating on ethanol-gasoline blends. In *SAE Technical Papers*; 2012.

(53) Chen, L.; Braisher, M.; Crossley, A.; Stone, R.; Richardson, D. The Influence of Ethanol Blends on Particulate Matter Emissions from Gasoline Direct Injection Engines. In *SAE Technical Papers*; 2010.

(54) Bruehlmann, S.; Forss, A.-M.; Steffen, D.; Heeb, N. V. Benzene: a secondary pollutant formed in the three-way catalyst. *Environ. Sci. Technol.* **2005**, *39* (1), 331–338.

(55) U.S. Department of Energy. Gas Mileage of 2013 Ford Focus https://www.fueleconomy.gov/feg/bymodel/2013_Ford_Focus.shtml.

(56) U.S. Department of Energy. Gas Mileage of 2004 Ford Focus https://www.fueleconomy.gov/feg/bymodel/2004_Ford_Focus.shtml.

(57) U.S. Department of Energy. Gas Mileage of 2008 Ford Focus https://www.fueleconomy.gov/feg/bymodel/2008_Ford_Focus.shtml.

(58) Seinfeld, J. H.; Pandis, S. N. Dynamics of Aerosol Populations. In *Atmospheric Chemistry and Physics: From Air Pollution to Climate Change*; John Wiley & Sons: Hoboken, 2006; pp 588–627.

(59) Sgro, L. A.; Sementa, P.; Vaglieco, B. M.; Rusciano, G.; D'Anna, A.; Minutolo, P. Investigating the origin of nuclei particles in GDI engine exhausts. *Combust. Flame* **2012**, *159* (4), 1687–1692.

(60) Stojkovic, B. D.; Fansler, T. D.; Drake, M. C.; Sick, V. High-speed imaging of OH* and soot temperature and concentration in a stratified-charge direct-injection gasoline engine. *Proc. Combust. Inst.* **2005**, *30 II* (2), 2657–2665.

(61) Velji, A.; Yeom, K.; Wagner, U.; Spicher, U.; Rossbach, M.; Suntz, R.; Bockhorn, H. Investigations of the formation and oxidation of soot inside a direct injection spark ignition engine using advanced laser-techniques. *SAE Tech. Pap.* **2010**, No. 2010-01-0352.

(62) Zimmerman, N.; Pant, P.; Jeong, C.-H.; Rais, K.; Delgado-Saborit, J. M.; Wallace, J. S.; Evans, G. J.; Brook, J. R.; Pollitt, K. J. Carbonaceous aerosol sampling of gasoline direct injection engine exhaust with an integrated organic gas and particle sampler. *Sci. Total Environ.* **2016** *in preparation.*

(63) May, A. A.; Presto, A. A.; Hennigan, C. J.; Nguyen, N. T.; Gordon, T. D.; Robinson, A. L. Gas-particle partitioning of primary organic aerosol emissions: (1) Gasoline vehicle exhaust. *Atmos. Environ.* **2013**, *77*, 128–139.

(64) Kamboures, M. A.; Hu, S.; Yu, Y.; Sandoval, J.; Rieger, P.; Huang, S.-M.; Zhang, S.; Dzhema, I.; Huo, D.; Ayala, A.; et al. Black carbon emissions in gasoline vehicle exhaust: A measurement and instrument comparison. *J. Air Waste Manage. Assoc.* **2013**, *63* (8), 886–901.

(65) Yelverton, T. L. B.; Hays, M. D.; Gullett, B. K.; Linak, W. P. Black carbon measurements of flame-generated soot as determined by optical, thermal-optical, direct absorption, and laser incandescence methods. *Environ. Eng. Sci.* **2014**, *31* (4), 209–215.

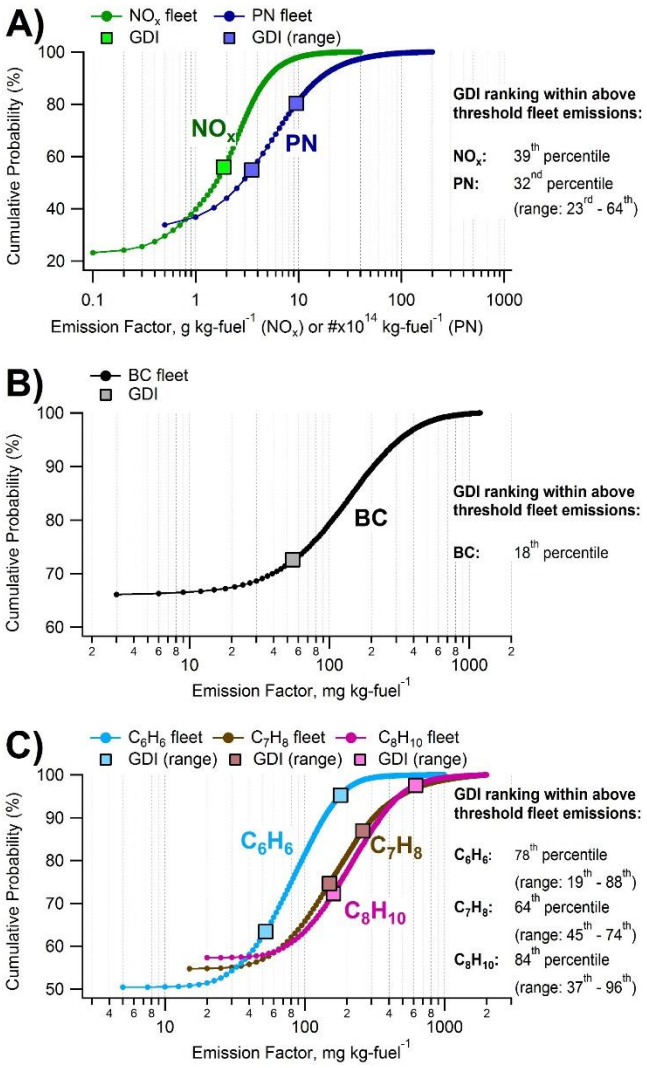

Figure 1: Cumulative probability distribution of Toronto fleet emission factors for PN and NOx (A), BC (B) and for VOCs (C) from Wang et al.[32]. The starting point of the distribution represents the fraction of below detection plumes. Overlaid on the fleet distributions are the GDI EFs from this study. To the right of each distribution the GDI ranking within the above threshold emissions (i.e., rank on the curve). If statistically significant differences between the seasons were observed, two markers indicating the range are shown, otherwise one average GDI EF is shown. Tabulated mean fleet and GDI EFs are provided in the Supporting Information. Fleet PN cut-off: 7 nm (Teledyne 651), GDI PN cut-off: 3 nm (TSI 3788).

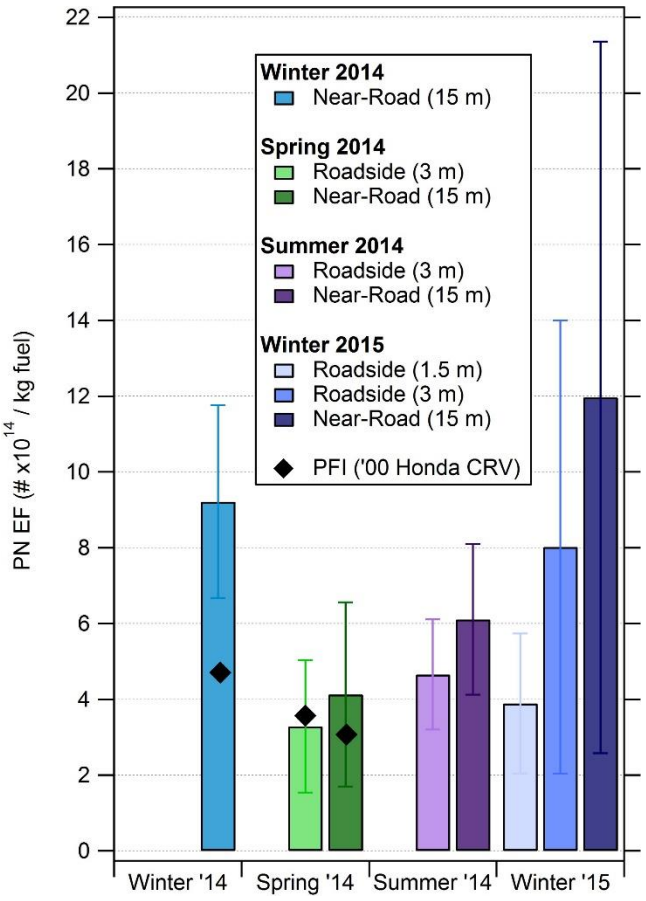

706

707 **Figure 2**: Average GDI particle number (PN) emission factors measured by the 3788 CPC (> 3nm) at the near-road
708 (15 m) and roadside (1.5 – 3 m) sites during the four measurement campaigns with 95% confidence intervals.

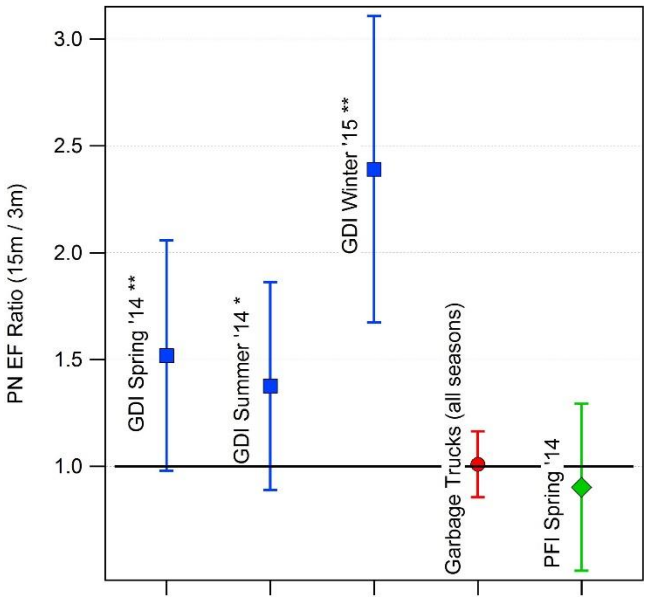

709

710 **Figure 3**: Average ratio of particle number emission factors measured by the 3788 CPC (> 3 nm) at the near-road (15
711 m) and roadside (3 m) site on a plume-by-plume basis for the spring 2014, summer 2014, and winter 2015 campaigns
712 (with 95% confidence intervals). Results were compared to diesel garbage truck plumes measured across the
713 measurement campaigns and PFI plumes measured in the spring 2014 campaign. Asterisks indicate p-values from a
714 one sample t-test with the null hypothesis $\mu_o = 1$. **: $p < 0.05$, *: $p < 0.1$

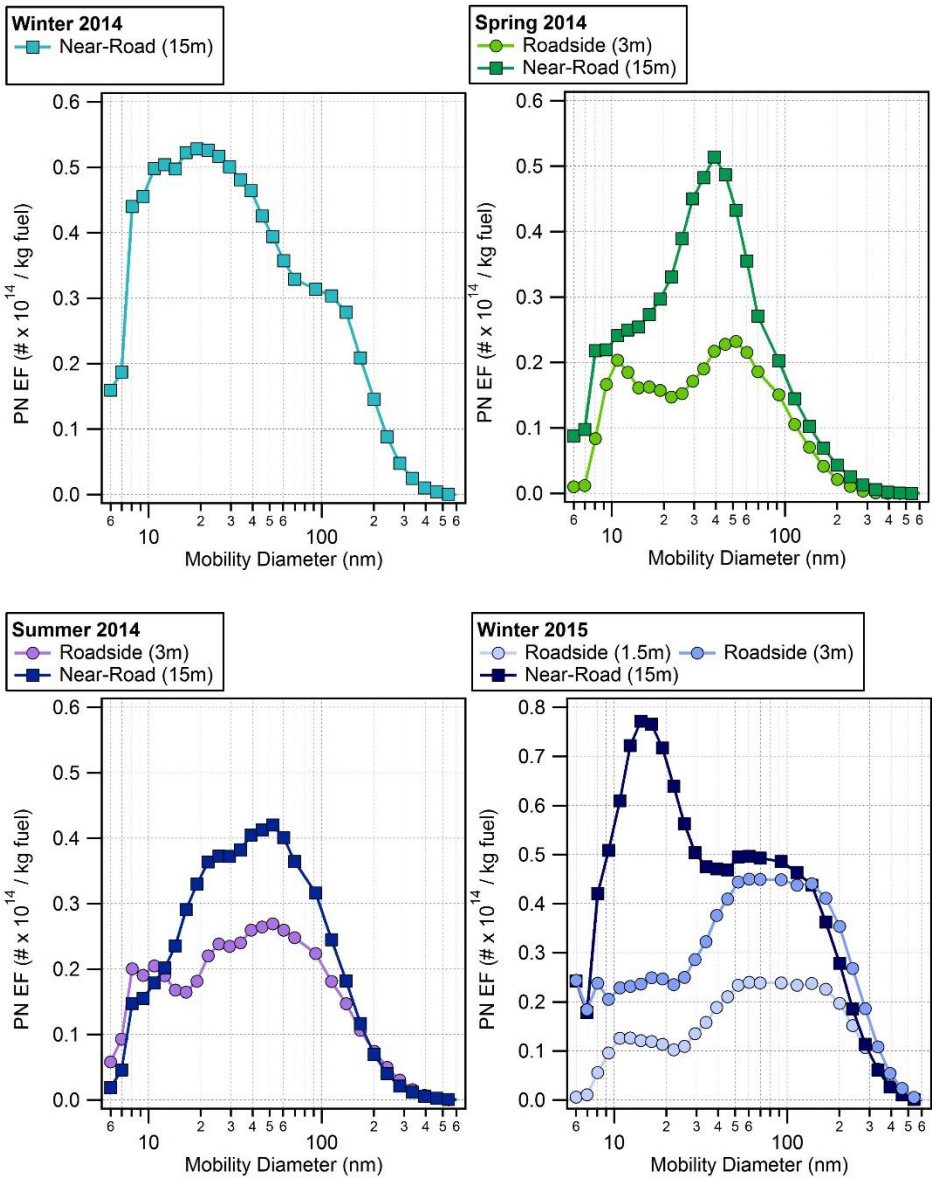

715

716 **Figure 4**: Size-resolved PN EFs at the near-road (15 m) and roadside (1.5 – 3 m) sites.

717

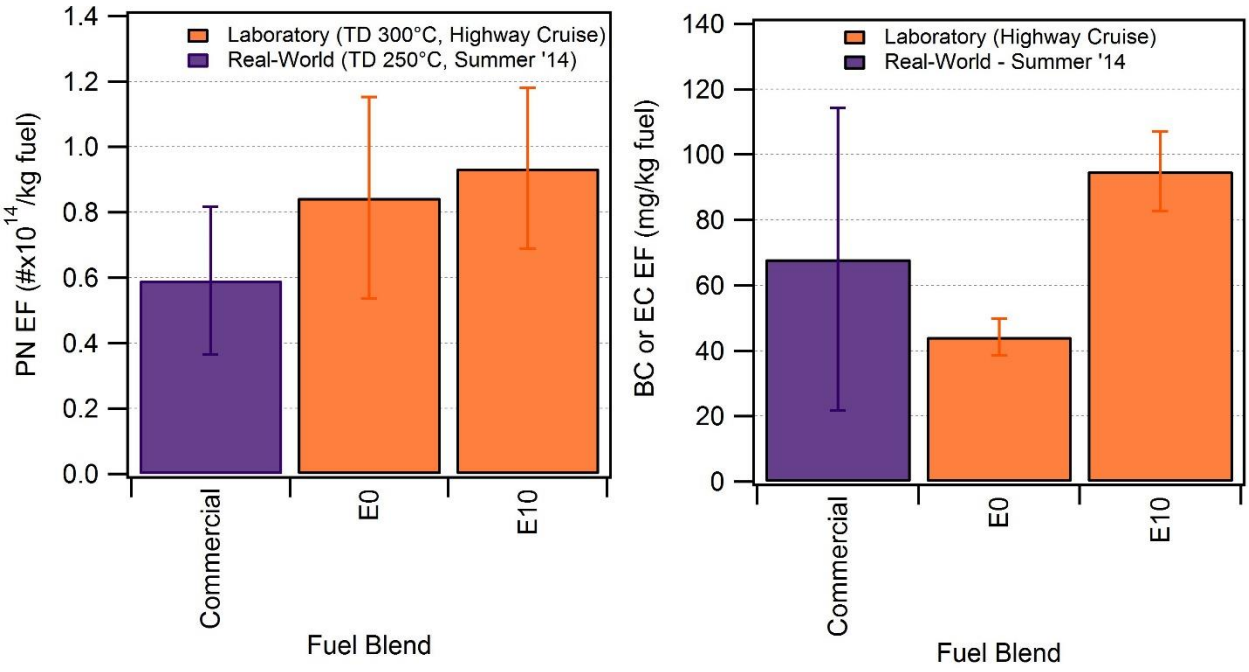

718

719 **Figure 5**: Average particle number emission factors measured in the laboratory for E0-E10 summer-grade fuels
720 (orange) during a simulated highway cruise operation (diluter T=300°C) (EEPS 3090, > 6 nm) and average
721 thermodenuded (250°C) particle number emission factor (CPC 3788, >3 nm) measured during the real-world in
722 summer 2014 (purple) (left panel), and average elemental carbon (EC) emission factors measured in the laboratory
723 for E0-E10 fuels (orange) during a simulated highway cruise operation and average black carbon (BC) emission
724 factors during the real-world in summer 2014 (purple) (left panel).

725